

A first appraisal of prognostic ocean DMS models and prospects for their use in climate models

Yvonnick Le Clainche,^{1,2} Alain Vézina,³ Maurice Levasseur,¹ Roger A. Cropp,⁴ Jim R. Gunson,⁵ Sergio M. Vallina,^{6,7} Meike Vogt,^{8,9} Christiane Lancelot,¹⁰ J. Icarus Allen,¹¹ Stephen D. Archer,¹¹ Laurent Bopp,¹² Clara Deal,¹³ Scott Elliott,¹⁴ Meibing Jin,¹³ Gill Malin,⁸ Véronique Schoemann,^{10,15} Rafel Simó,⁶ Katharina D. Six,¹⁶ and Jacqueline Stefels¹⁷

Received 5 November 2009; revised 3 April 2010; accepted 29 April 2010; published 15 September 2010.

[1] Ocean dimethylsulfide (DMS) produced by marine biota is the largest natural source of atmospheric sulfur, playing a major role in the formation and evolution of aerosols, and consequently affecting climate. Several dynamic process-based DMS models have been developed over the last decade, and work is progressing integrating them into climate models. Here we report on the first international comparison exercise of both 1D and 3D prognostic ocean DMS models. Four global 3D models were compared to global sea surface chlorophyll and DMS concentrations. Three local 1D models were compared to three different oceanic stations (BATS, DYFAMED, OSP) where available time series data offer seasonal coverage of chlorophyll and DMS variability. Two other 1D models were run at one site only. The major point of divergence among models, both within 3D and 1D models, relates to their ability to reproduce the summer peak in surface DMS concentrations usually observed at low to mid- latitudes. This significantly affects estimates of global DMS emissions predicted by the models. The inability of most models to capture this summer DMS maximum appears to be constrained by the basic structure of prognostic DMS models: dynamics of DMS and dimethylsulfoniopropionate (DMSP), the precursor of DMS, are slaved to the parent ecosystem models. Only the models which include environmental effects on DMS fluxes independently of ecological dynamics can reproduce this summer mismatch between chlorophyll and DMS. A major conclusion of this exercise is that prognostic DMS models need to give more weight to the direct impact of environmental forcing (e.g., irradiance) on DMS dynamics to decouple them from ecological processes.

Citation: Le Clainche, Y., et al. (2010), A first appraisal of prognostic ocean DMS models and prospects for their use in climate models, *Global Biogeochem. Cycles*, 24, GB3021, doi:10.1029/2009GB003721.

¹Québec-Océan, Département de Biologie, Université Laval, Québec, Canada.

²Now at Institut des Sciences de la Mer de Rimouski, Université du Québec à Rimouski, Rimouski, Canada.

³Bedford Institute of Oceanography, Fisheries and Oceans Canada, Dartmouth, Canada.

⁴Atmospheric Environment Research Centre, Griffith School of Environment, Griffith University, Nathan, Australia.

⁵CSIRO Marine and Atmospheric Research, Hobart, Tasmania, Australia.

⁶Institut de Ciències del Mar–Consejo Superior de Investigaciones Científicas, Barcelona, Spain.

⁷Now at Department of Earth, Atmospheric and Planetary Sciences, Massachusetts Institute of Technology, Cambridge, Massachusetts, USA.

⁸School of Environmental Sciences, University of East Anglia, Norwich, UK.

⁹Now at Environmental Physics, ETH Zurich, Zurich, Switzerland.

¹⁰Ecologie des Systèmes Aquatiques, Université Libre de Bruxelles, Brussels, Belgium.

¹¹Plymouth Marine Laboratory, Plymouth, UK.

¹²Laboratoire des Sciences du Climat et de l'Environnement, IPSL, Gif-sur-Yvette, France.

¹³International Arctic Research Center, University of Alaska Fairbanks, Fairbanks, Alaska, USA.

¹⁴Los Alamos National Laboratory, Los Alamos, New Mexico, USA.

¹⁵Now at Department of Biological Oceanography, Royal Netherlands Institute for Sea Research, Texel, Netherlands.

¹⁶Max Planck Institute for Meteorology, Hamburg, Germany.

¹⁷Department of Plant Ecophysiology, University of Groningen, Haren, Netherlands.

1. Introduction

[2] Sulfur plays a major role in the chemistry of the atmosphere, particularly the formation and evolution of aerosols, and consequently affects the earth's radiative balance and climate [IPCC, 2007]. Oceanic volatile sulfur gases, mainly in the form of biogenic dimethylsulfide (DMS) produced by marine plankton, are a major natural source of sulfur to the atmosphere [Andreae and Raemdonck, 1983; Bates *et al.*, 1992]. In the atmosphere, DMS is rapidly oxidized to form sulfur aerosols acting as cloud condensation nuclei (CCN) and altering the radiative transfer [Andreae and Crutzen, 1997]. DMS emissions are important to particle growth in the marine boundary layer and new particle formation in the free troposphere [Liss *et al.*, 1997]. With anthropogenic sulfur emissions declining [Stern, 2005], the relative importance of DMS to the atmospheric sulfur burden is increasing. This makes the integration of dynamic biogenic sulfur sources into climate models very important. Dynamic biogenic sulfur modules have already been embedded in ocean-atmosphere models, but they diverge widely in their structure and simulation capacity.

[3] Since the recognition of the role of ocean DMS emissions in climate [Charlson *et al.*, 1987], studies on DMS ocean dynamics have revealed an increasingly complex system involving all components of the marine food web, including phytoplankton, zooplankton, bacteria and viruses (Figure 1). While this complexity was (and still is) being revealed, models that attempt to incorporate ecological processes in dynamic descriptions of DMS(P) cycling have been proposed [Gabric *et al.*, 1993, 2001; Vézina, 2004]. Faced with the task of selecting variables and processes to be incorporated, modelers have made different choices and this has led to considerable variation in terms of structure (compartments included) and process representation (environmental and ecological controls on processes). Although empirical DMS models have been compared [Belviso *et al.*, 2004], no comparable evaluation of prognostic process-based DMS models has been attempted to date.

[4] Here we report on a first international comparison exercise of four global three-dimensional (3D) ocean and five local one-dimensional (1D) vertical water column process-based DMS models. Our objectives were to evaluate the ability of these models to reproduce observed spatial and temporal patterns in DMS concentrations, to identify and discuss the reasons for areas of divergence, and to recommend future directions for model development, observation and experimentation. The models and methods for simulation and model comparison are explained in section 2. In section 3, we first report basic results of the model comparisons and extract a pattern in the divergence among model simulations and their relationship to observations. We then introduce a theoretical stability analysis of generic prognostic process-based DMS model that explains this pattern and relate the pattern to previous empirical and experimental results. Finally, in section 4, we present implications of our results for global climate models.

2. Methods

2.1. Models Comparison Process

[5] CODiM, which stands for Comparison of Ocean Dimethylsulfide Models, is a multidisciplinary group set up in response to a call from the international SOLAS science plan and implementation strategy (see <http://www.solas-int.org/aboutsolas/organisationandstructure/sciplanimpstrategy/sciplanis.html>) for a comparison of process-based DMS models to accelerate progress in that area and to point to currently unmet research needs. Results presented in this paper were discussed during the first CODiM workshop, sponsored by the SOLAS Project Office, the Belgian Science Policy Office, and Canadian SOLAS, which took place in Brussels, Belgium, December 4–8 2006. More information on CODiM can be found at the following address at <http://www.quebec-ocean.ulaval.ca/CODiM>.

2.2. Models Description

[6] We compared both local one-dimensional (1D) and global three-dimensional (3D) process-based DMS models (Table 1). All nine models involved in this comparison exercise share the same basic structure: a physical model drives a carbon or nitrogen-based planktonic ecosystem model which in turn drives a model of sulfur cycling. There is no feedback from biology on physics or from biogenic sulfur cycling on carbon or nitrogen cycling in these models. The four 3D models are based on Ocean General Circulation Models that differ mostly in their spatial resolution (horizontal and vertical) and details of their atmospheric forcing. The five 1D models, except one which was forced offline, were coupled to the open source water column General Ocean Turbulence Model (GOTM 3.0, <http://www.gotm.net>). This approach provided uniform physical forcings to all the 1D ecosystem models.

[7] The models vary considerably in ecological complexity, with the number of explicit ecological compartments ranging from 2 in the simplest one to 10 in the most complex. Interestingly, the 3D and 1D models cover almost the same ecological complexity spectrum. The cell quotas of DMSP (dimethylsulfoniopropionate, DMS precursor) in phytoplankton vary by as much as 4 orders of magnitudes between taxa [Stefels *et al.*, 2007]. Accordingly, most models (7 out of 9) divide (implicitly in HAMOCC) the autotrophs into 2 to 4 phytoplankton functional types (PFTs) which are assigned different DMSP quotas. The two remaining models (NODEM2 and DMOS) use implicit representations of this variability in cell quota (shift toward higher DMSP quota in summer) as a function of environmental light intensity. On the other hand, three out of the four 3D models also include some variability in their PFTs quotas of DMSP as a function of light, nutrients and temperature. The representation of heterotrophic compartments is generally less complex, with the number of zooplankton compartments ranging between 1 and 3 and with only two 1D models (ERSEM-DMS and DMOS) having an explicit representation of bacteria. Most models use an implicit bacterial remineralization function which may be constant or variable as a function of temperature or other environmental factors.

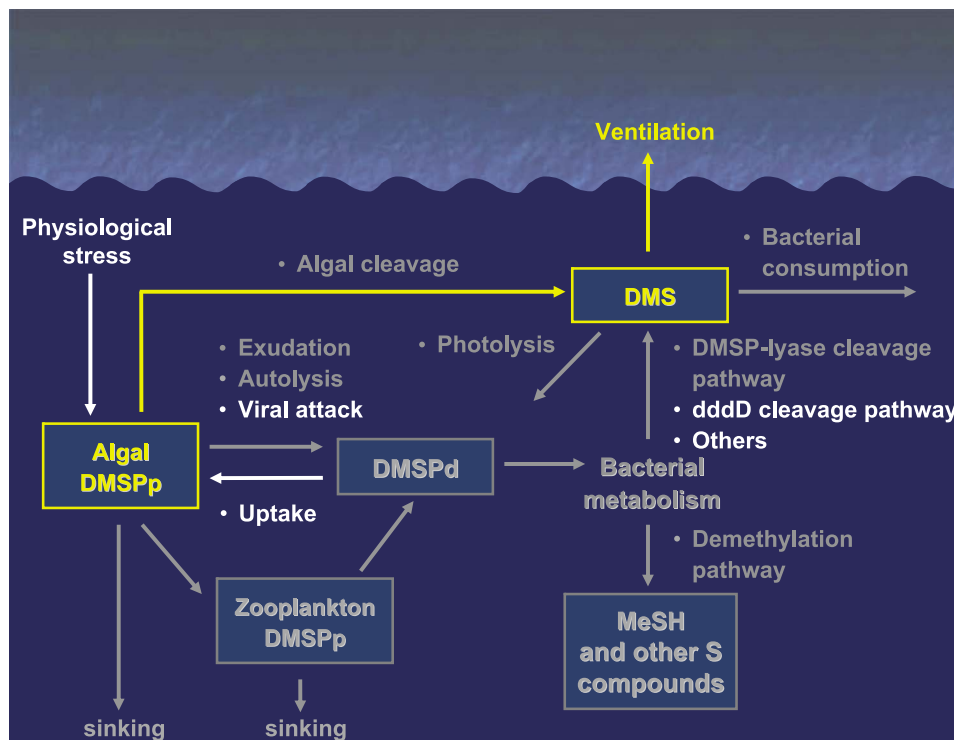


Figure 1. Schematic of the cycling of dimethylsulfide (DMS) and associated compounds (DMSPp, DMSPd, MeSH) in the surface ocean. Increases in knowledge over approximately 10-year intervals since the initial proposal that DMS influences climate are color-coded. Pools and pathways that were considered at the time of the original paper in 1987 [Charlson *et al.*, 1987] are shown in yellow. Additional pools and pathways that came to light by the next major review in 1996 [Kiene *et al.*, 1996] are portrayed in gray. Finally, new processes recognized since 1996 are depicted in white [Simó, 2001; Sunda *et al.*, 2002; Howard *et al.*, 2006; Malin, 2006; Vila-Costa *et al.*, 2006; Stefels *et al.*, 2007; Todd *et al.*, 2007]. DMSP is dimethylsulfoniopropionate, the precursor of DMS which is found either in particulate form inside organisms (subscript p) or free in the water (subscript d). MeSH is methanethiol, the end product of the demethylation pathway. DMSP-lyase and dddD designate alternative pathways for the conversion of DMSP into DMS. Physiological stress designates an ensemble of environmentally driven processes that can stimulate the production of DMSPp in algae (see text for details).

[8] With respect to DMS cycling, the majority of models (5 out of 9) involve 3 organic sulfur pools: particulate DMSP (DMSPp) bound to planktonic organisms, dissolved DMSP (DMSPd), and DMS [Gabric *et al.*, 2001; Vézina, 2004]. Although some models bypass the DMSPd pool and transform DMSPp directly into DMS (PISCES and PhEcoM-DMS) or explicitly represent only DMSPd and DMS (POP and HAMOCC), all the models basically depict the same processes implied in the DMS(P) cycle. DMSPp is released as dissolved DMSPd through a variety of processes, including exudation, grazing and mortality. Part of the DMSPd is transformed into DMS through bacterial metabolism that either demethylates DMSP to use it as a sulfur source or cleaves it enzymatically to use it as a carbon source and release DMS [Kiene *et al.*, 2000]. The DMSP to DMS transformation yield that represents the percentage of DMSPd that is routed to DMS is fixed in most models (6 out of 9), or depends on the bacterial DMSP consumption. Some models introduce other

direct DMS production terms, notably a direct DMS exudation from phytoplankton cells. DMS can in turn be removed through bacterial consumption, photo-oxidation and ventilation to the atmosphere. The representation of the role of bacteria in DMS(P) transformations varies greatly, primarily depending on how bacterial activity is represented in the ecological model, with only two 1D models having an explicit representation of bacteria. Although DMS photolysis is primarily driven by UV radiation [Toole *et al.*, 2003; Stefels *et al.*, 2007], this is still unresolved in all the models. Technical characteristics of DMS(P) cycle modeling in both 3D and 1D models are compiled in Tables 2 and 3, respectively.

2.3. Simulations and Comparisons With Data

[9] We compared the outputs of the global 3D models as they were provided by the participating scientists. No attempts were made to enforce uniformity in atmospheric forcing, spatial resolution, and physical schemes as this was

Table 1. The 3D and 1D Models Compared During This Study and Data Sets Used in the Comparison^a

	3D Models					1D Models				
	POP	PISCES	HAMOCC	PlankTOM	NODEM2	ERSEM-DMS	PhEcoM-DMS	DMOS	CMOC2-DMS	
Reference	<i>Elliott</i> [2009]	<i>Bopp et al.</i> [2008]	<i>Six and Maier-Reimer</i> [2006]	<i>Buitenhuis et al.</i> [2006]	<i>Le Clainche et al.</i> [2004]	<i>Archer et al.</i> [2004]	<i>Jodwalis et al.</i> [2000]	<i>Vallina et al.</i> [2008]	<i>Monahan and Denman</i> [2004]	
Physical model	POP	NEMO	LSG	OPA-ORCA	GOTM	GOTM	GOTM	Diagnostic based on GOTM	GOTM	
Horizontal resolution	3 × 3°	2° × 0.5° – 2°	3.5° × 3.5°	2° × 0.5° – 2°	n/a	n/a	n/a	n/a	n/a	
Vertical resolution	20 levels	31 levels	22 levels	31 levels	n/a	n/a	n/a	n/a	n/a	
Surface layer	12 m	10 m	50 m	10 m	1 m	1 m	1 m	1 m	1 m	
Atmospheric forcing	NCEP reanalysis	Various data sets	NCEP reanalysis	NCEP reanalysis	NCEP reanalysis	NCEP reanalysis	NCEP reanalysis	NCEP reanalysis	NCEP reanalysis	
Ecological complexity	4: P ₃ Z ₁ (P ₆ and B implicit)	4: P ₂ Z ₂ (B implicit)	2: P ₁ Z ₁ (P ₃ implicit)	5: P ₃ Z ₂ (B implicit)	2: P ₁ Z ₁	10: P ₄ Z ₃ B ₃	5: P ₂ Z ₃	3: P ₁ Z ₁ B ₁	4: P ₂ Z ₂	
DMS(P) complexity	2:DMSPd, DMS	2:DMSPp, DMS	2:DMSPd, DMS	3:DMSPp, DMSPd, DMS	3: DMSPp, DMSPd, DMS	3: DMSPp, DMSPd, DMS	2: DMSPp, DMS	3:DMSPp, DMSPd, DMS	3:DMSPp, DMSPd, DMS	
Effect of environment on DMS(P) fluxes?	Yes	Yes	No	Yes	Yes	No	No	Yes	No	
Effect independent of ecological dynamics?	Yes	No	No	No	Yes	No	No	Yes	No	
Data for comparison			<i>Global products: SeaWiFS chlorophyll a</i> <i>Surface DMS climatology</i>		<i>Stations: BATS, DYFAMED, OSP</i>	<i>Stations: BATS, DYFAMED, OSP</i>	<i>Stations: BATS, DYFAMED, OSP</i>	<i>Stations: BATS</i>	<i>Stations: OSP</i>	

^aThe name of the physical ocean model, its horizontal (n/a for 1D models) and vertical resolution, and the source of atmospheric forcing are listed for each model. Ecological complexity lists the number of explicit ecological compartments followed by a breakdown into phytoplankton (P_x), zooplankton (Z_y) and bacterial (B_z) compartments, where the subscript gives the number of compartments of each type. DMS(P) complexity shows the number of sulfur compounds resolved explicitly by the model. The majority of models (5 out of 9) include some stress functions which modulate the DMS(P) fluxes as a function of light, nutrients or temperature (effect of environment on DMS(P) fluxes), but only 3 models make these stress functions explicitly dependent on time (or space) –varying environmental factors (effect independent of ecological dynamics). This effectively decouples the DMS(P) production from the production in the parent ecological model (see text for more details). All global models are compared on the same global data products. Three out of the five 1D models are compared on all 3 oceanic stations, whereas the two others were run at one site only. More technical details on DMS(P) cycle modeling in the 3D and 1D models are available in Tables 2 and 3 respectively.

Table 2. Technical Characteristics of DMS(P) Cycle Modeling in the 3D Models Evaluated During This Study^a

Model Name	POP	PISCES	HAMOCC	PlankTOM
S(DMSP): C quota	Variable as function of nutrient and light stress, temperature and Chl <i>a</i> in each specific group (6)	- Fixed for diatoms; - Variable as function of nutrient and light stress for nanophytoplankton	Species-dependent constant	Variable as function of nutrient and light stress and temperature in each specific group (3)
Bacterial DMSPd consumption	Function of implicit bacterial biomass and DMSPd concentration	n/a	Function of temperature and DMSPd concentration (Michaelis-Menten uptake)	Function of temperature, implicit bacterial biomass and activity and DMSPd concentration (Michaelis-Menten uptake)
DMSP to DMS transformation yield	Fixed yield	Variable as function of bacterial nutrient stress	Fixed yield	Fixed yield
Other DMS production source	n/a	n/a	Fixed rate from phytoplankton degradation; Estimated direct <i>Phaeocystis</i> production from temperature and iron	- Additional fixed enzymatic DMSPd cleavage; Direct - DMS exudation
Bacterial DMS consumption	Function of implicit bacterial biomass and DMS concentration	Function of implicit bacterial biomass and activity and DMS concentration (Michaelis-Menten uptake)	Function of temperature and DMS concentration (Michaelis-Menten uptake)	Function of implicit bacterial biomass and activity and - DMS concentration (Michaelis-Menten uptake)
DMS photo-degradation	Function of PAR(z)	Function of PAR(z)	Function of PAR(z)	Function of PAR(z)
DMS surface ventilation	<i>Wanninkhof</i> [1992]	<i>Wanninkhof</i> [1992]	<i>Wanninkhof</i> [1992]	<i>Wanninkhof</i> [1992]

^aDOC is for Dissolved Organic Carbon, and PAR is for Photosynthetically Active Radiation.

Table 3. Technical Characteristics of DMS(P) Cycle Modeling in the 1D Models Evaluated During This Study^a

Model Name	NODEM2	ERSEM-DMS	PhEcoM-DMS	DMOS	CMOC2-DMS
S(DMSP): N quota	Variable in function of light	Fixed in each specific group (4)	Fixed in each specific group (2)	Variable in function of light	Fixed in each specific group (2)
Bacterial DMSPd consumption	Constant rate	Michaelis-Menten uptake by explicit specific DMSPd bacteria consumers	Constant rate directly applied on DMSPp compartment	Michaelis-Menten uptake by explicit bacteria	Constant rate
DMSP to DMS transformation yield	Fixed yield	Fixed yield	Fixed yield	Conditional DMS yield in function of bacteria demand	Fixed yield
Other DMS production source	No	Additional fixed enzymatic DMSPd cleavage	No	Additional direct DMS exudation from phytoplankton in function of light	No
Bacterial DMS consumption	Constant rate	Michaelis-Menten uptake by explicit specific DMS bacteria consumers	Constant rate	Michaelis-Menten uptake by explicit bacteria	Constant rate
DMS photo-degradation	Function of PAR(z)	Function of PAR(z)	Function of PAR(z)	Function of PAR(z)	Function of PAR(z)
DMS surface ventilation	<i>Nightingale et al.</i> [2000]	<i>Nightingale et al.</i> [2000]	<i>Nightingale et al.</i> [2000]	<i>Nightingale et al.</i> [2000]	<i>Wanninkhof</i> [1992]

^aDOC is for Dissolved Organic Carbon, and PAR is for Photosynthetically Active Radiation.

Table 4. Characteristics of the Time Period Simulated, the Hydrographic Data Sets Used to Run GOTM, and the Chl *a* and DMS(P) Data Sets Used in the 1D Ecosystem-DMS Model Comparison at Each of the Three Oceanic Stations^a

Station	Time Period Simulated	Temperature and Salinity Data	Chl <i>a</i> Data	DMS(P) Data
BATS (32°N, 64°W)	Jan. 1990 to Dec. 1994	Vertical profiles of T & S at Hydrostation S (32.1°N, 64.3°W) from 1989/11 to 1995/01 (~ every 10 days) [Kleypas and Doney, 2001]	Vertical profiles of [Chl <i>a</i>] at BATS from 1990/01 to 1995/01 (~ every month) [Kleypas and Doney, 2001]	Vertical profiles of [DMS], [DMSPp] and [DMSPd] at Hydrostation S (32.1°N, 64.3°W) from 1992/01 to 1994/11 (~ every 15 days) [Dacey et al., 1998]
DYFAMED (43°N, 8°E)	Jan. 1992 to Dec. 1995	Vertical profiles of T & S from 1991/12 to 1996/01 (~ every month) [Marty et al., 2002]	Vertical profiles of [TChl <i>a</i>] from 1991/01 to 1995/11 (~ every month) [Marty et al., 2002]	Vertical profiles of [DMSPP] and [DMS+DMSPd] from 1993/03 to 1995/02 (~ every month) [Belviso et al., 2001]
OSP (50°N, 145°W)	Jan. 2002 to Dec. 2003	Vertical profiles of T & S interpolated at OSP from Argo data from 2001/12 to 2004/02 (every 5 days) [Freeland and Cummins, 2005]	Vertical profiles of [Chl <i>a</i>] from 1996 to 2001 (~ 3 cruises per year) [Wong et al., 2005]	Vertical profiles of [DMS] from 1996 to 2001 (~ 3 cruises per year) [Wong et al., 2005] + vertical profiles of [DMS] and [DMSPp] in July 2002 [Levasseur et al., 2006]

^aAll the formatted data as well as the technical settings for GOTM simulations used in this study are available online on the CODiM website (<http://www.quebec-ocean.ulaval.ca/CODiM>).

clearly infeasible for these large complex models in the time available. The 3D model simulations were compared to global sea surface chlorophyll *a* (Chl *a*) concentration from the SeaWiFS climatology (<http://oceancolor.gsfc.nasa.gov/SeaWiFS>) and global surface DMS concentrations from both the *Kettle and Andreae* [2000] climatology used as reference and the NOAA DMS database (<http://saga.pmel.noaa.gov/dms>), which is an updated version of the database used by *Kettle and Andreae* [2000]. The outputs (surface Chl *a* and DMS) from the various models and the reference climatologies were first regridded onto a global (360° × 180°) regular 1° × 1° grid and then averaged zonally into 5° × 1 month bins to produce latitude-time (Hovmöller) diagrams. Spearman rank correlations were calculated between the binned model-predicted variables (surface Chl *a* and DMS) and reference climatologies as indicators of how closely the various models matched the reference patterns. In addition, we generated global maps of seasonal correlations between surface Chl *a* and surface DMS for reference climatologies and for results of each global 3D model using the following procedure [Vallina et al., 2007]: using a spatial running window of 7° × 7°, we obtained for every 1° × 1° grid box of the global ocean time series of 12 points (monthly values) of surface Chl *a* and surface DMS. Then, we calculated for every 1° × 1° grid box the seasonal Spearman correlation coefficient between the two variables (12 degrees of freedom), generating global maps of seasonal correlations.

[10] Three out of the five 1D ecosystem-DMS models were run for 3 different oceanic stations representing the subtropical North Atlantic (Bermuda Atlantic Time series Study, BATS, 32°N 64°W), the western Mediterranean (Dynamics of Atmospheric Fluxes in the MEDiterranean sea, DYFAMED, 43°N 8°E) and the subarctic northeast Pacific (Ocean Station Papa, OSP, 50°N 145°W), where time series data available offer seasonal coverage of chlorophyll *a* (Chl *a*) and DMS(P) variability. The two other 1D models were run at one site only (Table 1). The same settings for turbulence physics, site-specific atmospheric forcing and initial and restoring hydrographic conditions were used to run the 1D vertical column model GOTM, providing uniform physical forcing to all the 1D ecosystem-DMS models (Table 4).

[11] For each site, the surface net solar radiation, the surface heat fluxes, the surface momentum fluxes and the meteorological fields (6h interval) used to force GOTM were extracted from the NOAA NCEP-NCAR Climate Data Assimilation System 1 reanalysis [Kalnay et al., 1996]. Hydrographic (temperature and salinity) data were also assembled for each site and used for GOTM initialization and relaxation (Table 4). Simulations at BATS and DYFAMED were run from 1990 to 1994 and from 1992 to 1995 respectively. We analyzed only the last 3 years of these simulations for which DMS(P) observations were available for comparison. DMS(P) data were collected approximately bi-weekly from Jan 1992 to Nov 1994 at Hydrostation S (32°10'N, 64°30'W) close to BATS [Dacey et al., 1998] and monthly from Mar 1993 to Feb 1995 at DYFAMED [Belviso et al., 2001]. For OSP, we assembled DMS(P) and Chl *a* data collected from 1996 to 2002 (on average 3 cruises per year) [Wong et al., 2005; Levasseur et al., 2006] to build a refer-

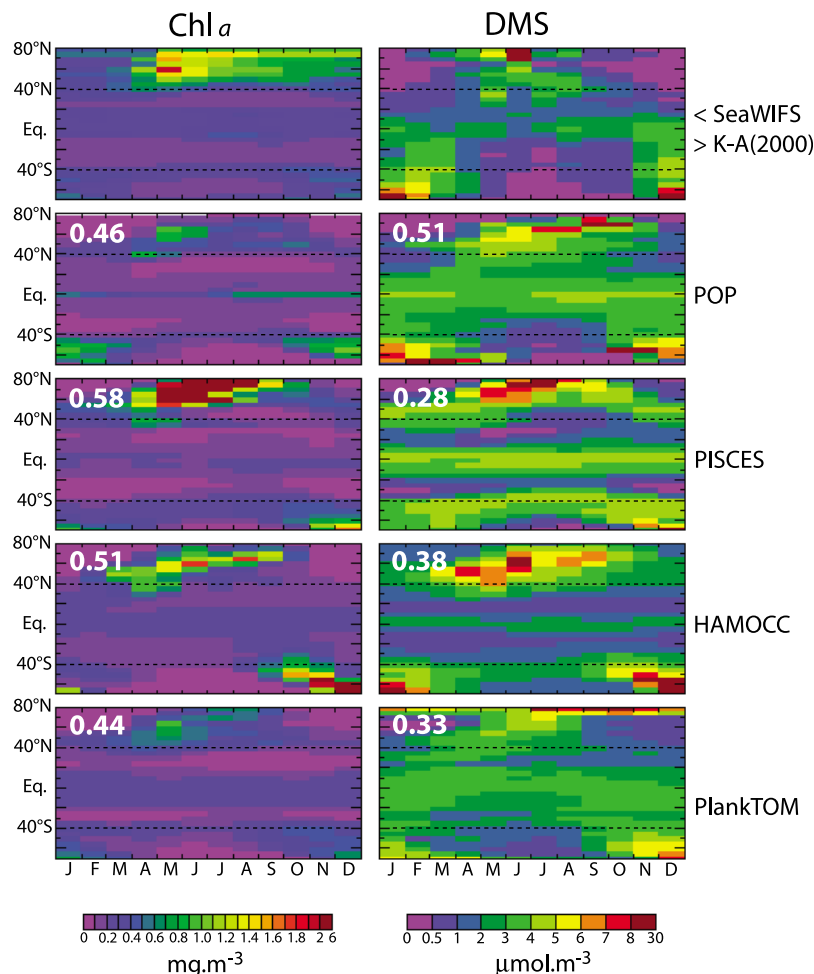


Figure 2. Latitude-time (Hovmöller) plots of (top row) climatologies and (following rows) results from 4 global models for (left column) chlorophyll a (Chl a) ($\text{mg} \cdot \text{m}^{-3}$) and (right column) DMS ($\mu\text{mol} \cdot \text{m}^{-3}$). Data were binned and averaged in 5° latitude \times 1 month boxes and are displayed here from 70°S to 80°N on a linear color scale. Models are identified in Table 1. Numbers in the upper left-hand corner of each model plot are the Spearman rank correlations between the variables (Chl a or DMS) simulated by the corresponding model and the SeaWiFS or *Kettle and Andreae* [2000] climatologies represented in the top panels.

ence mean seasonal cycle. Simulations at OSP were run for 2002 and 2003 using the temperature and salinity data interpolated at OSP from Argo data [Freeland and Cummins, 2005] for GOTM initialization and relaxation. First year of simulation (2002) was repeated once as setup, but we kept only the second occurrence in the analysis. Table 4 sums up all the data sets used in the 1D models comparison. The outputs (Chl a , DMSPp and DMS) of the various models and the reference data were averaged over the upper ocean mixed layer (determined as the depth where the temperature is 0.5°C below the surface temperature) and for four seasonal periods of three months (the first one starting in January). The 1D models were originally calibrated to diverse locations and were intentionally not re-calibrated to fit the specific characteristics of the new locations where they were applied. Our objective was not to find the best exportable model but to

learn from the different dynamics they displayed on the same data set.

3. Results and Discussion

3.1. Model Comparisons

[12] Turning first to the global models, we note that they all capture the prominent spring-summer bloom in northern latitudes (north of 40°N) and reproduce the pattern of Chl a minima in subtropical gyres separated by a weak maximum at the equator (Figure 2). All global models show the zonal pattern in Chl a with distinct seasonal regimes at low and mid-to-high latitudes, although POP and PlankTOM simulate lower Chl a levels overall. Spearman correlations between the simulated Chl a and SeaWiFS (at a $5^\circ \times 1$ month resolution) are roughly similar ranging between 0.44 and 0.58, confirming

the visual impression that models are comparable in terms of their ability to simulate Chl *a* (see Figure S1).¹ In terms of DMS, all the models reproduce the pattern of higher DMS during spring–summer at high northern and southern latitudes (Figure 2). The models diverge mostly in how they represent DMS structures at mid- to low latitudes. The climatology suggests meridional patterns with DMS summer maxima in both hemispheres, coinciding with Chl *a* minima. POP, and to a lesser extent PlankTOM, approximate this pattern whereas PISCES and HAMOCC produce zonal fields that follow more closely those of Chl *a*. The patterns observed in these latitude–time (Hovmöller) maps may be partly biased by averaging across basins. However, a close examination of the data show that in spite of some differences among ocean basins, the mismatch between the Chl *a* pattern and the DMS during summer is still present. Spearman correlations between the simulated DMS concentrations and the *Kettle and Andreae* [2000] climatology (at a $5^\circ \times 1$ month resolution) are more variable than in the case of Chl *a* and range between 0.23 and 0.5 (Figure 2), with the POP model having the highest correlation. POP is also the model that best captures the shift from positive seasonal correlations between Chl *a* and DMS at mid- to high latitudes to negative correlation at low to midlatitudes (Figure 3). The correlations between the NOAA DMS database and model predictions are weaker (0.14 to 0.41, with POP and PlankTOM giving the highest correlations) (see Figure S2). The models produce DMS global emissions ranging from 24 to 31 TgS/yr, with HAMOCC and POP giving the highest values (Table 5). This compares well with estimated global emissions of 15–33 TgS/yr [*Kettle and Andreae*, 2000]. Summarizing, the global dynamic models show more consistent skill at simulating Chl *a* than DMS; POP was best able to capture some of the features of the DMS climatologies, followed by PlankTOM, even though these models are not superior to the other models at simulating Chl *a*.

[13] With respect to the 1D model applications, BATS provides the most complete data set for comparison. For that station, all 1D models simulate essentially equivalent predictions of seasonally averaged Chl *a* in the surface mixed layer (Figure 4). However, there are significant differences in simulated DMS, with some models underestimating the summer concentrations as is also seen in the 3D simulations at low latitudes. The same models also strongly under-predict DMSPp during the summer period when Chl *a* is progressively declining. Only NODEM2 and DMOS capture the seasonal reversal between Chl *a* and DMS. They are also the only models that approximate the high summer DMS emissions at BATS inferred from the measured concentrations and wind speed (Table 6). A similar pattern is evident at DYFAMED, although here no DMS data are available (DMS and DMSPd were not measured separately), leaving only DMSPp data for the comparison. NODEM2 comes closest to capturing the summer rise in DMSPp at DYFAMED. The situation is different at OSP where DMS is an order of magnitude higher in summer than in winter, while Chl *a* slightly increases from winter–spring to summer (instead of

declining as at the other two stations). At this station, all the models (with the exception of NODEM2) successfully capture the summer increase in biomass, but diverge considerably in their predictions of Chl *a*, with ERSEM–DMS and CMOC2–DMS providing the closest matches to the observed seasonal pattern. However, only CMOC2–DMS shows the clear DMS(P) increase that is observed during summer.

3.2. Mathematical Considerations on Model Structure

[14] We conclude from the model comparisons that a major point of divergence among models, both within 3D and 1D models, relates to their ability to reproduce the summer peak in DMS concentrations usually observed at low to mid- latitudes, a phenomena referred to as the ‘DMS summer paradox’ [*Simó and Pedrós-Alió*, 1999]. The inability of most models to capture this summer DMS maximum appears to be constrained by the basic structure of prognostic DMS models. The basis for this conclusion is explained in the following stability analysis.

[15] The current state of knowledge of the DMS cycle in the ocean can be expressed by a set of autonomous differential equations composed of production and loss terms that has the following generic form:

$$\frac{dDMSP}{dt} = f_1(k_1; P, Z, B, \dots) - f_2(k_2; DMSP, \dots) \quad (1)$$

$$\frac{dDMS}{dt} = f_3(k_3; DMSP, P, Z, B, \dots) - f_4(k_4; DMS, \dots) \quad (2)$$

where P, Z, B, \dots are the concentrations of the state variables of the ecosystem model, DMSP and DMS are the concentrations of these compounds, f_i (with $i = 1, \dots, 4$) represent the functional relationships between DMSP and DMS and the state variables of the ecosystem model, and k_i (with $i = 1, \dots, 4$) represent sets of the rate parameters associated with the production or loss processes.

[16] The ellipses (...) represent other ecosystem state variables (but not DMSP or DMS) and reflect that DMS models may differ in the components included explicitly in functions f_i . However, there are several important ways in which all models agree:

[17] 1. DMSP does not appear in f_1 and DMS does not appear in f_3 , that is, all models are consistent in that DMSP and DMS will not increase in concentration if no living biota is present (i.e., no production of DMSP from DMSP and no production of DMS from DMS).

[18] 2. DMS does not appear in f_2 , that is, all models are consistent in that losses in DMSP are independent of DMS concentrations.

[19] 3. The loss terms for DMSP and DMS include terms that are functions of DMSP or DMS respectively.

[20] These autonomous DMS models will have one steady state:

$$DMSP^* = f_1, f_2(k_1, k_2; P, Z, B, \dots) \quad (3)$$

$$DMS^* = f_3, f_4(k_3, k_4; DMSP^*, P, Z, B, \dots) \quad (4)$$

¹Auxiliary materials are available with the HTML. doi:10.1029/2009GB003721.

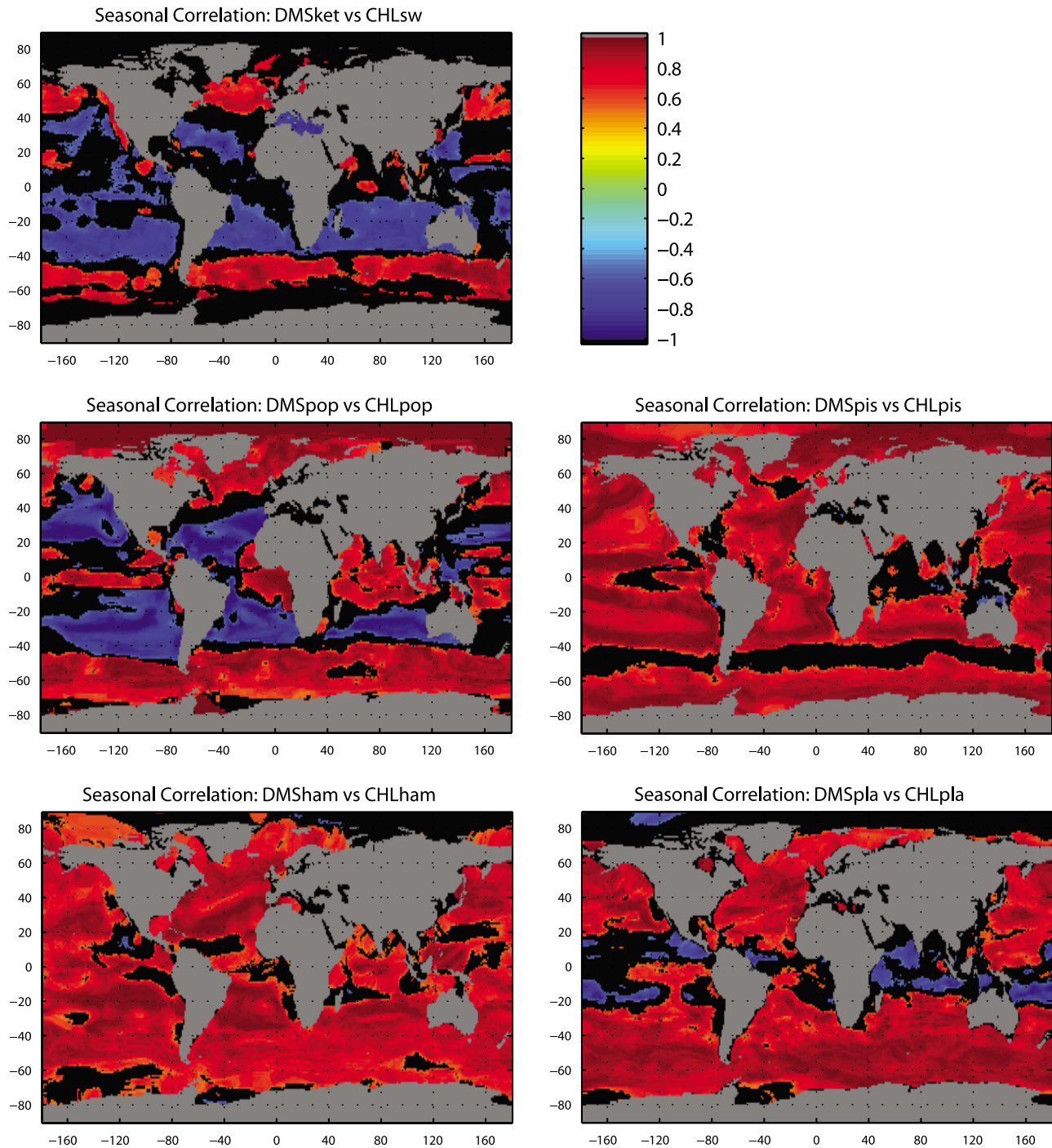


Figure 3. Seasonal correlations between surface DMS and surface Chl *a* concentrations on a $360^{\circ} \times 180^{\circ}$ grid for the world ocean based on (top, DMSket vs CHLsw) the *Kettle and Andreae* [2000] and SeaWiFS climatologies and then on (middle and bottom) results of each global model (DMSxxx vs CHLxxx, where model abbreviations xxx are pop for POP, pis for PISCES, pla for PlankTOM, and ham for HAMOCC). Significant correlations at 95% confidence level for $|r| > 0.5$ and at 80% confidence level for $|r| > 0.4$.

As DMS^* appears within the steady state expression for DMS, it is further possible to write the steady state DMS^* concentration solely as a function of the ecosystem state variables and parameters.

[21] A Lyapunov stability analysis [Jordan and Smith, 1999] of the system (equations (1) and (2)) indicates that the steady state given by equations (3) and (4) is always an

Table 5. Global DMS Sea-to-Air Flux^a

Climatology	POP	PISCES	HAMOCC	PlankTOM
15–33	31	20	31	24

^aUnits are Tg S/year. Estimated from climatology [Kettle and Andreae, 2000] and predicted by global models, using the Wanninkhof [1992] formulation.

asymptotically stable node, and always has eigenvalues of the form:

$$\lambda_1 = -\hat{f}_2(\hat{k}_2)$$

$$\lambda_2 = -\hat{f}_4(\hat{k}_4)$$

where the circumflex (^) indicates a subset of the original. The eigenvalues are inversely related to the time that the DMS system takes to return to its steady state after a perturbation. DMS models typically have negative eigenvalues that are in the order of 1–10 times the magnitude of phytoplankton growth rates. This suggests that they will return to steady state very rapidly compared to the dynamics of the ecosystem models [Cropp *et al.*, 2004].

[22] This analysis reveals that DMS and DMSP dynamics are slaved to the parent ecosystem models, that is, the sulfur model stays at or close to steady state, with the steady state concentration values being determined by the dynamics of the ecosystem models. The degree of positive correlations between Chl *a* and DMS will depend on the weightings assigned to production of DMS by the various ecosystem components, but the slaving of the sulfur models to the

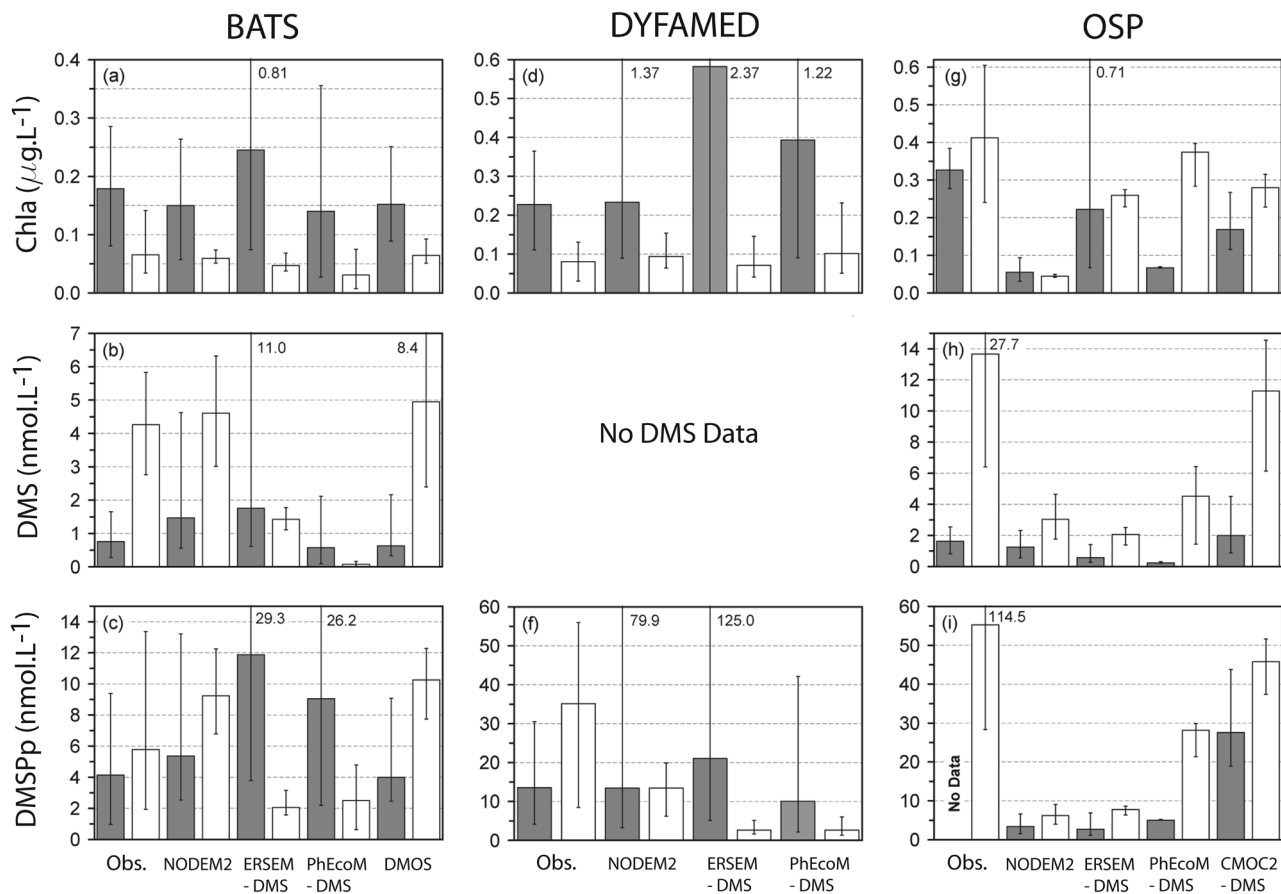


Figure 4. Concentrations of (top) Chl *a* ($\mu\text{g} \cdot \text{L}^{-1}$), (middle) DMS ($\text{nmol} \cdot \text{L}^{-1}$), and (bottom) particulate DMSP ($\text{nmol} \cdot \text{L}^{-1}$) depth-averaged over the surface mixed layer and time-averaged over winter-spring (January–February–March – gray columns) and summer (July–August–September – white columns) seasons at stations BATS, DYFAMED and OSP. For each panel, the first pair of bars (noted Obs.) show the observed data, while the 4 other pairs of bars show the results simulated by the different 1D DMS-ecosystem models used (see Table 1 for model identification). Note that DMS was not available for DYFAMED. The error bars are minima and maxima for each seasonal period and include both the variability within a season for one particular year and the inter-annual differences between 1992 and 94 for BATS, 1993–95 for DYFAMED, and 1996–2002 for OSP. The mixed layer depth was diagnosed as the depth where the temperature is 0.5°C under the surface temperature.

Table 6. Annual Mean, Winter Season Mean, and Summer Season Mean Daily DMS Sea-to-Air Flux at BATS^a

	Calculated From DMS Data	NODEM2	ERSEM-DMS	PhEcoM-DMS	DMOS
Annual mean	5.24	7.40	4.90	1.52	4.59
Winter (JFM) mean	3.53	7.26	9.09	4.49	4.14
Summer (JAS) mean	6.03	5.65	1.99	0.08	5.29

^aUnits are $\mu\text{mol m}^{-2} \text{d}^{-1}$. Calculated from the DMS time series data [Dacey *et al.*, 1998] and predicted by 1D models, using the Nightingale *et al.* [2000] formulation.

ecosystem models is likely to explain much of the positive correlations between Chl *a* and DMS obtained by models under most ocean regimes.

3.3. Interpretation

[23] The biological turnover rate of DMSP (and hence DMS production) is short (hours to days) with respect to the spatiotemporal DMS-Chl *a* mismatch, which is of the order of 2–3 months. Introducing ecological succession from DMSPp-poor to DMSPp-rich phytoplankton species during the transition from the winter-spring bloom to the summer stable period can stretch the lag in the models to a few weeks, but generally not long enough to match the observed lag. However, the stability analysis above suggests that the mismatch may be reproduced by applying an environmental forcing directly to the DMS(P) production and cycling terms, freeing them from complete dependence on the parent ecological model. Only 3 models (POP, NODEM2, and DMOS) include direct effects of environment on DMS(P) fluxes that are explicitly dependent on time (or space)-varying environmental factors and thus independent of ecological dynamics (Table 1). NODEM2 and DMOS do include separate forcing terms for DMS(P) production and cycling, while POP explicitly fits DMS(P) cycling terms to large scale spatial patterns in DMS. As a consequence, these models achieve greater success in simulating the summer mismatch. Two global models (PISCES and PlankTOM) also include some stress functions which modulate the DMS(P) fluxes as a function of light, nutrients or temperature (see Tables 1 and 2), although not as independently of ecological dynamics as POP, and as a result their DMS simulations remain more closely coupled to ecological processes.

[24] The finding that a direct environmental forcing is important is supported by recent evidence that DMSPp production and DMS release by autotrophs could be directly stimulated by environmental stresses such as UV radiation or nutrient limitation (the anti-oxidant hypothesis) or that increased DMSPp production could result from metabolic overflow during photosynthesis [Sunda *et al.*, 2002; Stefels *et al.*, 2007]. All three of the models (POP, NODEM2 and DMOS) that include independent effect of environment factors use irradiance as an external forcing term for their DMS (P) modules, echoing a recent finding that DMS concentrations at local to global scales can be predicted empirically from the solar radiation dose in the upper mixed layer [Vallina and Simó, 2007]. Despite the fact that both NODEM2 and DMOS use irradiance as external forcing, they diverge in how they simulate DMS production increase in summer. In DMOS, DMS is directly produced by phytoplankton exu-

dition as a function of light [Vallina *et al.*, 2008], whereas no direct DMS production from phytoplankton is included in NODEM2 (Table 3). A recent 1D modeling study in Sargasso Sea [Toole *et al.*, 2008] uses a direct UVR-induced DMS release similar to that in DMOS to reproduce the summer upper-ocean DMS concentrations.

[25] Our model comparison points to DMSPp production and release in the water as critical processes that are currently not well represented in dynamic sulfur cycle models. These processes include increased DMSP synthesis in algal cells and/or DMS release from algal cells under stress conditions (e.g., high light and nutrient limitation), light-dependent DMSP to DMS conversion by bacteria, and DMSP-lyase activity in some algal groups. These processes should receive more attention in further observational/experimental work and model development. These developments are also promising from a modeling point of view because they facilitate the critical decoupling between Chl *a* and DMS. This is not to mean that the decoupling and seasonal timing are the only issues with DMS(P) models. The inclusion of UV radiation effects on DMS cycle (on DMS loss by photolysis notably), and more generally on ecosystem dynamics is an important issue for future ecosystem-DMS model developments.

[26] The results we obtained at OSP clearly indicate that, under some ocean regimes, improvements in the ecological models may be more important. In that case, the best ecological model in the sense of simulating the best seasonal cycle of plankton biomass for that station also showed the best match to the seasonal DMS variability without using any stress function (Table 1). This was recently confirmed by Steiner and Denman [2008] who succeeded in simulating DMS seasonal cycle at OSP using the same 1D ecosystem model as CMOC2-DMS coupled with a more complex DMS(P) model without any stress function. However, they also showed that increasing DMS yield under UV stress slightly improved their model's performance. On the other hand, the decoupling issue and its possible causes can only be addressed by investigating and modeling the cycling of biogenic sulfur itself. Progress on this may help resolve some of the complexities in sulfur cycling and provide workable solutions for climate modelers to parameterize marine DMS emissions.

4. Implications for Climate Models

[27] The problems that current process-based DMS models have reproducing the summer mismatch between Chl *a* and DMS has significant implications for climate models. Although the mismatch in sulfur levels involved might seem

small, the areas where these patterns occur are vast (roughly between the 10 to 40 degree latitude belts). Hence, eliminating the subtropical summer maxima would decrease global DMS emissions by up to 15%. The underestimation of the modeled summer DMS flux may be even higher if summer DMS maxima are not limited to subtropical regimes. The latitude-season mapping (Figure 2) suggests that, even though Chl *a* and DMS are correlated at mid- to high latitudes (Figure 3), their seasonal evolution are different. The meridional pattern of summer DMS peaks stretches from pole to equator in both hemispheres, as expected from recent findings that DMS concentrations are tightly related to solar radiation dose [Vallina and Simó, 2007]. Local studies reinforce this view. Summer DMS maxima are also observed in temperate Mediterranean waters (e.g., Microbial Observatory of Blanes Bay, [Vila-Costa et al., 2007]) and other coastal waters (e.g., English coast off Plymouth, [Archer et al., 2009]). Capturing these seasonal phenomena in climate models is critical because of the short lifetime of DMS in the atmosphere [Andreae and Crutzen, 1997] and the important contribution of summer DMS emissions to cloud-forming DMS oxidation products [Vallina et al., 2007], especially in the marine boundary layer.

[28] Large scale process-based models are unlikely to improve in the absence of targeted laboratory studies and field data. In assessing the models, we repeatedly faced the situation that we are comparing simulations to interpolations of sparse data. The NOAA database is an invaluable resource that requires maintenance and extension. We know that not all DMS measurements enter the database, and that the methods used to acquire those that are already there may have their own flaws (e.g., potential overestimation of DMSPd) [Kiene and Slezak, 2006]. An updated version of the global surface DMS concentrations climatology is currently under process within an international Surface Ocean Lower Atmosphere Study project, but more generally a coordinated international effort is needed to improve the spatial and temporal resolution of the climatology by increasing systematic and time series collections of DMS data in under-sampled ocean regimes.

[29] **Acknowledgments.** We thank Surface Ocean Lower Atmosphere Study (SOLAS) and the Belgian Federal Science Policy Office for supporting the workshop. Support for participation of individual participants was provided by the National Sciences and Engineering Research Council of Canada and the Canadian Foundation for Climate and Atmospheric Sciences, the U.K. Natural Environmental Research Council Advanced Research Fellowship, the North Pacific Research Board Project, the European Research and Training Network GREENCYCLES, the Australian Research Council, the EU 6th Framework Programme, the U.S. Department of Energy Office of Biology and Environmental Research and the Spanish MEC. Finally, we thank everyone in the DMS community who has contributed data to the Global Surface Seawater Dimethylsulfide (DMS) Database.

References

Andreae, M. O., and P. J. Crutzen (1997), Atmospheric aerosols: Biogeochemical sources and role in atmospheric chemistry, *Science*, 276, 1052–1058, doi:10.1126/science.276.5315.1052.

Andreae, M. O., and H. Raemdonck (1983), Dimethyl sulfide in the surface ocean and the marine atmosphere: A global view, *Science*, 221, 744–747, doi:10.1126/science.221.4612.744.

Archer, S. D., F. J. Gilbert, J. I. Allen, J. Blackford, and P. D. Nightingale (2004), Modelling the seasonal patterns of dimethylsulfide production

and fate during 1989 at a site in the North Sea, *Can. J. Fish. Aquat. Sci.*, 61(5), 765–787, doi:10.1139/f04-028.

Archer, S. D., D. G. Cummings, C. A. Llewellyn, and J. R. Fishwick (2009), Phytoplankton taxa, irradiance and nutrient availability determine the seasonal cycle of DMSP in temperate shelf seas, *Mar. Ecol. Prog. Ser.*, 394, 111–124, doi:10.3354/meps08284.

Bates, T. S., B. K. Lamb, A. Guenther, J. Dignon, and R. E. Stoiber (1992), Sulfur emissions to the atmosphere from natural sources, *J. Atmos. Chem.*, 14(1–4), 315–337, doi:10.1007/BF00115242.

Belviso, S., H. Claustre, and J.-C. Marty (2001), Evaluation of the utility of chemo-taxonomic pigments as a surrogate for particulate DMSP, *Limnol. Oceanogr.*, 46, 989–995, doi:10.4319/lo.2001.46.4.0989.

Belviso, S., L. Bopp, C. Moulin, J. C. Orr, T. R. Anderson, O. Aumont, S. Chu, S. Elliott, M. E. Maltrud, and R. Simó (2004), Comparison of global climatological maps of sea surface dimethylsulfide, *Global Biogeochem. Cycles*, 18, GB3013, doi:10.1029/2003GB002193.

Bopp, L., O. Aumont, S. Belviso, and S. Blain (2008), Modeling the effect of iron fertilization on dimethylsulfide emissions in the Southern Ocean, *Deep Sea Res. Part II*, 55, doi:10.1016/j.dsr2.2007.12.002.

Buitenhuis, E., C. Le Quéré, O. Aumont, A. Beaugrand, A. Bunker, A. Hirst, T. Ikeda, T. O'Brien, S. Piontkovski, and D. Straile (2006), Biogeochemical fluxes through mesozooplankton, *Global Biogeochem. Cycles*, 20, GB2003, doi:10.1029/2005GB002511.

Charlson, R. J., J. E. Lovelock, M. O. Andreae, and S. G. Warren (1987), Oceanic phytoplankton, atmospheric sulphur, cloud albedo and climate, *Nature*, 326, 655–661, doi:10.1038/326655a0.

Cropp, R. A., J. Norbury, A. J. Gabric, and R. D. Braddock (2004), Modeling dimethylsulphide production in the upper ocean, *Global Biogeochem. Cycles*, 18, GB3005, doi:10.1029/2003GB002126.

Dacey, J. W. H., F. A. Howse, A. F. Michaels, and S. G. Wakeham (1998), Temporal variability of dimethylsulfide and dimethylsulfoniopropionate in the Sargasso Sea, *Deep Sea Res., Part I*, 45(1), 2085–2104, doi:10.1016/S0967-0637(98)00048-X.

Elliott, S. (2009), Dependence of DMS global sea-air flux distribution on transfer velocity and concentration field type, *J. Geophys. Res.*, 114, G02001, doi:10.1029/2008JG000710.

Freeland, H. J., and P. F. Cummins (2005), Argo: A new tool for environmental monitoring and assessment of the world's oceans, an example from the N.E. Pacific, *Prog. Oceanogr.*, 64(1), 31–44, doi:10.1016/j.pocean.2004.11.002.

Gabric, A., N. Murray, L. Stone, and M. A. Kohl (1993), Modelling the production of dimethylsulfide during a phytoplankton bloom, *J. Geophys. Res.*, 98(C12), 22,805–22,816, doi:10.1029/93JC01773.

Gabric, A., W. Gregg, R. Najjar, D. Erickson, and P. Matrai (2001), Modeling the biogeochemical cycle of dimethylsulfide in the upper ocean: A review, *Chemosph. Global Change Sci.*, 3, 377–392, doi:10.1016/S1465-9972(01)00018-6.

Howard, E. C., et al. (2006), Bacterial taxa that limit sulfur flux from the ocean, *Science*, 314, 649–652, doi:10.1126/science.1130657.

IPCC (2007), *Climate Change 2007: The Physical Science Basis. Contribution of Working Group I to the Fourth Assessment Report of the Intergovernmental Panel on Climate Change*, edited by S. Solomon et al., Cambridge Univ. Press, Cambridge, U. K.

Jodwalis, C. M., R. L. Benner, and D. L. Eslinger (2000), Modeling of dimethyl sulfide ocean mixing, biological production and sea-to-air flux for high latitudes, *J. Geophys. Res.*, 105(D11), 14,387–14,399, doi:10.1029/2000JD900023.

Jordan, D. W., and P. Smith (1999), *Nonlinear Ordinary Differential Equations*, 3rd ed., 560 pp., Oxford Univ. Press, Oxford, U. K.

Kalnay, E., et al. (1996), The NCEP/NCAR 40-year reanalysis project, *Bull. Am. Meteorol. Soc.*, 77(3), 437–472, doi:10.1175/1520-0477(1996)077<0437:TNYRP>2.0.CO;2.

Kettle, A. J. and M. O. Andreae (2000), Flux of dimethylsulfide from the oceans: A comparison of updated data sets and flux models, *J. Geophys. Res.*, 105(D22), 26,793–26,808, doi:10.1029/2000JD900252.

Kiene, R. P., and D. Slezak (2006), Low dissolved DMSP concentrations in seawater revealed by small-volume gravity filtration and dialysis sampling, *Limnol. Oceanogr. Methods*, 4, 80.

Kiene, R. P., P. T. Visscher, G. O. Kirst, and M. D. Keller (Eds.) (1996), *Biological and Environmental Chemistry of DMSP and Related Sulfonium Compounds*, Plenum Publ., New York.

Kiene, R. P., L. J. Linn, and J. A. Bruton (2000), New and important roles for DMSP in marine microbial communities, *J. Sea Res.*, 43, 209–224, doi:10.1016/S1385-1101(00)00023-X.

Kleypas, J. A., and S. C. Doney (2001), *Nutrients, Chlorophyll, Primary Production and Related Biogeochemical Properties in the Ocean Mixed Layer: A Compilation of Data Collected at Nine JGOFS Sites, NCAR*

- Tech. Note NCAR/TN-447+STR, 55 pp., Natl. Cent. for Atmos. Res., Boulder, Colo.
- Le Clainche, Y., M. Lévassieur, A. Vézina, J. W. H. Dacey, and F. J. Saucier (2004), Behaviour of the ocean DMS(P) pools in the Sargasso Sea viewed in a coupled physical-biogeochemical ocean model, *Can. J. Fish. Aquat. Sci.*, *61*(5), 788–803, doi:10.1139/f04-027.
- Lévassieur, M., et al. (2006), DMSP and DMS dynamics during a mesoscale iron fertilization experiment in the northeast Pacific. Part I. Temporal and vertical distributions, *Deep Sea Res., Part II*, *53*(20–22), 2353–2369, doi:10.1016/j.dsr2.2006.05.023.
- Liss, P. S., A. D. Hatton, G. Malin, P. D. Nightingale, and S. M. Turner (1997), Marine sulphur emissions, *Philos. Trans. R. Soc. Ser. B*, *352*, 159–169.
- Malin, G. (2006), New pieces of the marine sulfur cycle jigsaw, *Science*, *314*, 607–608, doi:10.1126/science.1133279.
- Marty, J.-C., J. Chiaverini, M.-D. Pizay, and B. Avril (2002), Seasonal and interannual dynamics of nutrients and phytoplankton pigments in the western Mediterranean Sea at the DYFAMED time-series station (1991–1999), *Deep Sea Res. Part II*, *49*(11).
- Monahan, A. H., and K. L. Denman (2004), Impacts of atmospheric variability on a coupled upper-ocean ecosystem model of the subarctic northeast Pacific, *Global Biogeochem. Cycles*, *18*, GB2010, doi:10.1029/2003GB002100.
- Nightingale, P. D., G. Malin, C. S. Law, A. J. Watson, P. S. Liss, M. I. Liddicoat, J. Boutin, and R. C. Upstill-Goddard (2000), In situ evaluation of air-sea gas exchange parameterizations using novel conservative and volatile tracers, *Global Biogeochem. Cycles*, *14*(1), 373–387, doi:10.1029/1999GB900091.
- Simó, R. (2001), Production of atmospheric sulfur by oceanic plankton: Biogeochemical, ecological and evolutionary links, *Trends Ecol. Evol.*, *16*, 287–294, doi:10.1016/S0169-5347(01)02152-8.
- Simó, R., and C. Pedrós-Alió (1999), Role of vertical mixing in controlling the oceanic production of dimethyl sulphide, *Nature*, *402*, 396–399, doi:10.1038/46516.
- Six, K. D., and E. Maier-Reimer (2006), What controls the oceanic dimethylsulfide (DMS) cycle? A modeling approach, *Global Biogeochem. Cycles*, *20*, GB4011, doi:10.1029/2005GB002674.
- Stefels, J., M. Steinke, S. M. Turner, G. Malin, and S. Belviso (2007), Environmental constraints on the production and removal of the climatically active gas dimethylsulphide (DMS) and implications for ecosystem modeling, *Biogeochemistry*, *83*(1–3), 245–275, doi:10.1007/s10533-007-9091-5.
- Steiner, N., and K. Denman (2008), Parameter sensitivities in a 1-D model for DMS and sulphur cycling in the upper ocean, *Deep Sea Res., Part I*, *55*, 847–865, doi:10.1016/j.dsr.2008.02.010.
- Stern, D. I. (2005), Global sulfur emissions from 1850 to 2000, *Chemosphere*, *58*, 163–175, doi:10.1016/j.chemosphere.2004.08.022.
- Sunda, W., D. J. Kieber, R. P. Kiene, and S. Huntsman (2002), An antioxidant function for DMSP and DMS in marine algae, *Nature*, *418*, 317–320, doi:10.1038/nature00851.
- Todd, J. D., R. Rogers, Y. G. Li, M. Wexler, P. L. Bond, L. Sun, A. R. J. Curson, G. Malin, M. Steinke, and A. W. B. Johnston (2007), Structural and regulatory genes required to make the gas dimethyl sulfide in bacteria, *Science*, *315*, 666–669, doi:10.1126/science.1135370.
- Toole, D. A., D. J. Kieber, R. P. Kiene, D. A. Siegel, and N. B. Nelson (2003), Photolysis and the dimethylsulfide (DMS) summer paradox in the Sargasso Sea, *Limnol. Oceanogr.*, *48*, 1088–1100, doi:10.4319/lo.2003.48.3.1088.
- Toole, D. A., D. A. Siegel, and S. C. Doney (2008), A light-driven, one-dimensional dimethylsulfide biogeochemical cycling model for the Sargasso Sea, *J. Geophys. Res.*, *113*, G02009, doi:10.1029/2007JG000426.
- Vallina, S., and R. Simó (2007), Strong relationship between DMS and the solar radiation dose over the global surface ocean, *Science*, *315*, 506–508, doi:10.1126/science.1133680.
- Vallina, S. M., R. Simó, S. Gasso, C. de Boyer-Montégut, E. del Río, E. Jurado, and J. Dachs (2007), Analysis of a potential “solar radiation dose-dimethylsulfide-cloud condensation nuclei” link from globally mapped seasonal correlations, *Global Biogeochem. Cycles*, *21*, GB2004, doi:10.1029/2006GB002787.
- Vallina, S. M., R. Simó, T. R. Anderson, A. Gabric, R. Cropp, and J. M. Pacheco (2008), A dynamic model of oceanic sulfur (DMOS) applied to the Sargasso Sea: Simulating the dimethylsulfide (DMS) summer-paradox, *J. Geophys. Res.*, *113*, G01009, doi:10.1029/2007JG000415.
- Vézina, A. F. (2004), Ecosystem modelling of the cycling of marine dimethylsulfide: A review of current approaches and of the potential for extrapolation to global scales, *Can. J. Fish. Aquat. Sci.*, *61*, 845–856, doi:10.1139/f04-025.
- Vila-Costa, M., R. Simó, H. Harada, J. M. Gasol, D. Slezak, and R. P. Kiene (2006), Dimethylsulfoniopropionate uptake by marine phytoplankton, *Science*, *314*, 652–654, doi:10.1126/science.1131043.
- Vila-Costa, M., J. Pinhassi, C. Alonso, J. Pernthaler, and R. Simó (2007), An annual cycle of dimethylsulfoniopropionate-sulfur and leucine assimilating bacterioplankton in the coastal NW Mediterranean, *Environ. Microbiol.*, *9*, 2451–2463, doi:10.1111/j.1462-2920.2007.01363.x.
- Wanninkhof, R. (1992), Relationship between wind speed and gas exchange over the ocean, *J. Geophys. Res.*, *97*(C5), 7373–7382, doi:10.1029/92JC00188.
- Wong, C.-S., S. E. Wong, W. A. Richardson, G. E. Smith, M. D. Arychuk, and J. S. Page (2005), Temporal and spatial distribution of dimethylsulfide in the subarctic northeast Pacific Ocean: A high-nutrient–low-chlorophyll region, *Tellus, Ser. B*, *57*(4), 317–331, doi:10.1111/j.1600-0889.2005.00156.x.
- J. I. Allen and S. D. Archer, Plymouth Marine Laboratory, Prospect Place, the Hoe, Plymouth PL1 3DH, UK.
- L. Bopp, LSCE, IPSL, Gif-sur-Yvette F-91191, France.
- R. A. Cropp, Atmospheric Environment Research Centre, Griffith School of Environment, Griffith University, Environment 1 Bldg. (N55) 0.28, 170 Kessels Rd., Nathan QLD 4111, Australia.
- C. Deal and M. Jin, IARC, University of Alaska Fairbanks, PO Box 757340, Fairbanks 99775-7340, AK, USA.
- S. Elliott, Los Alamos National Laboratory, PO Box 1663, Los Alamos, NM 87545, USA.
- J. R. Gunson, CSIRO Marine and Atmospheric Research, Castray Esplanade, Hobart TAS 7000, Australia.
- C. Lancelot, Ecologie des Systèmes Aquatiques, Université Libre de Bruxelles, Campus de la plain, Accès 3, Bât. A, local 1A3 207 (1er étage), Blvd. du triomphe, B-1050 Bruxelles, Belgium.
- Y. Le Clainche, ISMER, Université du Québec à Rimouski, Rimouski, Canada. (yvonnick_leclainche@uqar.ca)
- M. Lévassieur, Québec-Océan, Département de Biologie, Université Laval, 1045 ave. de la Médecine, Local 2078, Québec G1V 0A6, Canada.
- G. Malin and M. Vogt, School of Environmental Sciences, University of East Anglia, Norwich NR4 7TJ, UK.
- V. Schoemann, Department of Biological Oceanography, Royal Netherlands Institute for Sea Research, NL-1790 AB Texel, Netherlands.
- R. Simó and S. M. Vallina, ICM-CSIC, E-08003 Barcelona, Spain.
- K. D. Six, Max Planck Institute for Meteorology, Bundestr. 53, D-20146 Hamburg, Germany.
- J. Stefels, Department of Plant Ecophysiology, University of Groningen, PO Box 14, NL-9750 AA Haren, Netherlands.
- Dr., Vézina, BIO, Fisheries and Oceans Canada, PO Box 1006, 1 Challenger Dr., Dartmouth NS B2Y 4A2, Canada.